Int J Environ Res (2022) 16:27
https://doi.org/10.1007/s41742-022-00397-7

RESEARCH PAPER

Time Trends and Persistence in US Sea Level Data: An Investigation Using Fractional Integration Methods

Guglielmo Maria Caporale[1] · Luis A. Gil-Alana[2] · L. Sauci[3]

Received: 28 September 2021 / Revised: 13 February 2022 / Accepted: 18 February 2022

Abstract

This paper analyses US sea level data using long memory and fractional integration methods. Specifically, monthly data for 41 US stations covering the period from January 1950 to December 2018 are examined. Fractional integration methods suggest that all series exhibit orders of integration in the interval (0, 1), which implies long-range dependence with positive values of the differencing parameter; further, significant positive time trends are found in the case of 29 stations located on the East Coast and the Gulf of Mexico, and negative ones in the case of four stations on the North West Coast, but none for the remaining 8 on the West Coast. The highest degree of persistence is found for the West Coast stations and the lowest for the East Coast ones. Thus, in the event of shocks, more decisive action is required in the case of West Coast stations for the series to revert to their original trend.

Article Highlights

- **This paper analyses US sea level data using fractional integration.**
- **All series exhibit long-range dependence.**
- **Significant positive time trends are found in the East Coast and the Gulf of Mexico.**
- **Negative ones in the North West Coast.**
- **The highest degree of persistence is found for the West Coast and the lowest for the East Coast.**

Keywords Sea level · Time trends · Fractional integration

Introduction

In the last few decades, considerable efforts have been made to gain a deeper understanding of the effects of global climatic variations on the sea level, which is essential to prevent potential coastal flood hazards and mitigate their socio-economic and environmental consequences. Of particular interest are the Assessment Reports of the Intergovernmental Panel on Climate Change (IPCC). The empirical evidence from the First Assessment Report (FAR) published in 1990 to the most recent IPCC work (Oppenheimer 2019) indicates that there has been a global mean sea level (GMSL) rise of 1.0–2.0 mm year^{-1} during the twentieth century, which is much larger than in the previous two centuries (Warrick and Oerlemans 1990), and in the last two millennia as a whole (IPCC 2014: 4). In particular, the GMSL rise estimated from tide gauge data is of 1.5 [1.1–1.9] mm year^{-1}, with an acceleration range of [− 0.002–0.019] over the period 1902–2010, while the revised estimate from satellite altimetry data is 3.16 [2.79–3.53] mm year^{-1}, with an acceleration of 0.084 [0.059–0.090] mm year^{-1} over 1993–2015 (see Church et al. 2013; WCRP Global Sea Level Budget Group 2018; Oppenheimer et al. 2019).

However, this increase has not been uniform around the world. In particular, in the case of the US, there are important differences between the Eastern and Western coastline. The National Oceanic and Atmospheric Administration

✉ Luis A. Gil-Alana
alana@unav.es

[1] Department of Economics and Finance, Brunel University London, Uxbridge UB8 3PH, UK

[2] Department of Economics, Faculty of Economics and NCID, University of Navarra, 31009 Pamplona, Spain

[3] Department of Economics, UNIR, International University of La Rioja, 26006 Logroño, Spain

Published online: 07 April 2022

(NOAA), in its technical report NOS CO-OPS 053 (Zervas 2009) examined the linear mean sea level trends in 128 stations located on the US Atlantic and Pacific coasts, Alaska and the Gulf of Mexico, among other areas. According to this report, the upward trend in the regional sea level for the majority of the East coast stations implies a rate of increase above the twentieth century GMSL rise of 1.7 mm year^{-1}, the highest value (6.05 mm year^{-1}) being estimated for the Chesapeake Bay Bridge Tunnel station. By contrast, in the case of the West coast, the increase is around or below the GMSL rise of 1.7 mm year^{-1}. The highest regional sea levels increases have been observed in Louisiana, Eastern Texas and the stretch from Virginia to New Jersey, which can be explained by Gulf Stream variations, land subsidence and tectonic movements (Zervas 2009; Sweet et al. 2017).

Future scenarios for the sea level rise are based on emissions and the associated risks. It is expected that GMSL will continue increasing during the twenty-first century with mean values of 0.43 m [0.29–0.59], 0.55 [0.39–0.72] and 0.84 [0.61–1.10] for the Representative Concentration Pathway models (RCP)2.6, RCP4.5 and RCP8.5, respectively. Sweet et al. (2017) updated the future scenarios for the GMSL rise presented in Parris et al. (2012), and specified six possible 2100 scenarios ranging from 0.3 m (Low) to 2.5 m (Extreme). More specifically, in the Intermediate-High (1.5-m GMSL rise) scenario, the (high-low) increase would be 0.4–0.7 m (higher than the GMSL rise) for the US East Coast and 0.2–0.3 m (higher than the GMSL rise) for the West Coast.

All the available empirical evidence suggests a continuing upward trend in the sea level despite possible future reductions of anthropogenic emissions, which since 1970 have been the key factor determining ocean warming (Church et al. 2001; Oppenheimer et al. 2019). Hence, it is vital to gain further insights into this issue that can contribute to an effective decision-making and design of government policies. For this purpose, given the long-memory property characterising most geophysical and climatological time series—see, e.g., Percival et al. 2001; Gil-Alana, 2006, 2015, 2017; Ercan et al. 2013; Bunde 2017; Yuan et al. 2013, 2019), this paper applies a fractional integration approach to obtain new findings on sea level trends for different tide gauge stations on the US coastline. The layout of the paper is the following: Sect. 2 provides a brief review of the relevant literature; Sect. 3 describes the data and the methodology; Sect. 4 presents the empirical results; Sect. 5 offers some concluding remarks.

Literature Review

The analysis of sea level trends provides useful information about its variability in the past, present and future. Multiple factors can drive global and regional sea level changes such as atmospheric and ocean warming, tectonic dynamics or anthropogenic forces. In particular, recent studies point to ocean-thermal expansion, glaciers and the Greenland and Antarctic ice sheets and terrestrial water store, as the main factors behind the GMSL rise during the twentieth century and in the present (Warrick and Oerlemans 1990; Church et al. 2013; Church and Gregory 2019; Oppenheimer et al. 2019). There is an ongoing debate about the possible 'acceleration-deceleration' (Church and White 2006; Woodworth et al. 2009; Houston and Dean 2011; Boon 2012; Jevrejeva et al. 2014; Visser et al. 2015; Boon and Mitchell 2015; Watson 2016; etc.) or the 'intrinsic/natural-anthropogenic' nature of sea level changes (Jevrejeva et al. 2009; Lennartz and Bunde, 2012; Becker et al. 2014; Dangendorf et al. 2014, 2015; Slangen et al. 2016; Marcos et al. 2016; etc.); on the whole, it appears that anthropogenic factors have been the main cause of the sea level rise since 1970 (Oppenheimer et al. 2019).

Sea level variability is a complex issue that should be analysed carefully given the limitations of tide gauge and satellite altimetry data and the variety of applicable statistical techniques. The most common approach is trend analysis. Comprehensive surveys are provided by Mudelsee (2010), Chandler and Scott (2011) and Visser et al. (2015), who classify existing studies as using parametric, nonparametric or stochastic trend models, respectively.[1] Regarding this last approach, stochastic long-memory processes appear to be the most appropriate for geophysical/climate time series, since these tend to exhibit long-run dependence (LRD) or temporal correlations (Beran, 1994; Percival et al. 2001; Gil-Alana, 2006; Ercan et al. 2013; Graves et al. 2017). Such models range from those proposed by Hurst (1951) in hydrology, and later by Mandelbrot (1967) and Mandelbrot and Van Ness (1968) for self-similarity and the fractal dimension, to the AutoRegressive Fractionally Integrated Moving Average (ARFIMA) model of Granger and Joyeux (1980), and its subsequent extensions.

Long-memory models have been widely used for climate variables such as temperature (Bloomfield, 1992; Caballero et al. 2002; Franzke, 2012; Gil-Alana, 2005, 2008, 2018), but less for sea level data. In particular, there is very limited evidence concerning US tide gauge records. Jiang and Plotnick (1998) were the first to carry out fractal analysis

[1] Other papers estimating sea-level rise are Dangendorf et al. (2017), Kulp and Strauss (2019), Restrepo et al. (2021) and Zemunik et al. (2021).

using US coastline data with a continental dimension; applying the divider method (Mandelbrot 1982), they found more complexity in terms of the fractal dimension for the Atlantic coast, and also a significant correlation with latitudes, less complexity characterising lower latitudes. The fractal dimension ranges for Atlantic and Pacific shorelines are [1.0–1.70] and [1.0–1.27], respectively; in particular, Chesapeake Bay, the St. Johns River of Florida, and the Florida Keys, in the Atlantic coast, exhibit most complexity. Barbosa et al. (2008) considered 16 North Atlantic stations; employing three statistical approaches (parametric stationary tests, wavelet analysis and Generalized Least Squares (GLS)), they found LRD in all cases except Newlyn; in particular, they detected high persistence for Portland, Boston, Newport and New York that might reflect local/regional differences, as in the case of Chesapeake Bay (Kiptopeke, Hampton), which is characterised by subsidence and tectonic movements. However, according to Koop (2013), the rate of US mid-Atlantic sea level rise is within its historical variability.

In another recent study, Dangendorf et al. (2014) investigated sea level changes using 60 monthly average tide gauge records around the world. Their results from the Detrended Fluctuation Analysis-DFA2-(Kantelhardt et al. 2001) show, for all records, a LRD up to 35 years, which suggests the importance of the internal behaviour to understand sea level changes. By contrast, Becker et al. (2014) concluded that global and regional sea level changes are strongly driven by anthropogenic forces, in particular, in the case of New York, Baltimore and San Diego. Finally, Royston et al. (2018) addressed the issue of residual noise when estimating linear trends, and showed that it is coloured but non-AR(1) in the majority of cases, the AR(1) model being more appropriate for shorter series (Bos et al. 2014). The inclusion of climate indices in the regression does not affect the choice of noise model: for San Francisco and Seattle, the preferred noise models are ARFIMA specifications, with a trend coefficient (including climate indices) of 2.37 and 2.71, respectively, while for Honolulu, the preferred model is the Generalized Gauss Markov (GGM) noise model, with an estimated trend coefficient of 1.29. The study by Royston et al. (2018) is the closest to ours, since we also consider long-range dependence models based on fractional integration and estimate the time trend coefficients allowing the errors to be fractionally integrated.

Data and Methodology

We examine monthly tide gauge data over the period from January 1950 to December 2018 (828 observations per series) for 41 US stations located along most of its coastline. Specifically, we use the "Revised Local Reference (RLR)" data set from the Permanent Service for Mean Sea Level-PSMSL-(Holgate et al. 2013; PSMSL 2019); this includes some series which were originally annual but have been converted into monthly.

The fractional integration approach we use is more general than others such as ARMA/ARIMA models since it does not restrict the difference parameter to take an integer value. The standard approach estimates a linear time trend in the following regression model:

$$y_t = \alpha + \beta t + x_t \tag{1}$$

where a significant slope coefficient β implies the presence of a trend (positive or negative, depending on the sign of the coefficient). However, this set-up implicitly assumes that the error term, x_t is integrated of order 0 or $I(0)$0.2[2] This implies not only that it must be covariance-stationary, but also that the infinite sum of its autocovariances must be finite. This property is satisfied by the classical ARMA-type of models. If it is not, for example if the data display a high degree of persistence, first differences are then taken, on the assumption that x_t is integrated of order 1 or $I(1)$. Thus, x_t is specified such that $(1-B)x_t = u_t$, where B is the backshift operator ($Bx_t = x_{t-1}$) and u_t is $I(0)$. However, as already mentioned in Sect. 2, it is well known that many time series, especially climatological ones, are neither $I(0)$ nor $I(1)$ but $I(\mathrm{d})$ where d is a fractional value. This is approach taken in the present study.

Specifically, we estimate the time trend coefficient β and the fractional differencing parameter d (along with the other parameters) in the following regression model:

$$y_t = \alpha + \beta t + x_t, (1-B)^d x_t = u_t, u_t = \rho u_{t-12} + \varepsilon_t \tag{2}$$

where y_t is the observed time series; α and β are unknown coefficients, namely the intercept (constant) and the linear time trend coefficient; x_t stands for the regression errors, assumed to be $I(\mathrm{d})$, which implies that u_t is $I(0)$; moreover, given the possible seasonality of the monthly data analysed, a seasonal (monthly) AR(1) process is assumed for the $I(0)$ disturbances u_t, where ρ is the seasonality indicator.

Note that for the specific case where d in (2) is not an integer value, the following Binomial expansion can be used for $(1-B)^d$:

$$(1-B)^d = \sum_{j=0}^{\infty} \binom{d}{j} (-1)^j B^j = 1 - dB + \frac{d(d-1)}{2} B^2 - \ldots,$$

and thus

[2] For instance, in the classical Mann–Kendall trend test, the data should have no serial correlation, which is an even stronger asusmption that I(0).

Table 1 Time series examined and abbreviations

Series	Name	% of observed data
10_SF	10_SAN FRANCISCO	100.00%
12_NY	12_NEW YORK (THE BATTERY)	98.79%
112_FEB	112_FERNANDINA BEACH	96.13%
127_STT	127_SEATLE	99.87%
135_PHI	135_PHILADELPHIA (PIER 9 N)	97.46%
148_BAL	148_BALTIMORE	99.63%
155_HON	155_HONOLULU	100.00%
158_SDG	158_SAN DIEGO (QUARANTINE STATION)	98.065
180_ATL	180_ATLANTIC CITY	92.14%
183_POR	183_PORTLAND (MAINE)	99.63%
188_KW	188_KEY WEST	98.79%
225_KET	225_KETCHIKAN	98.42%
234_CHA	234_CHARLESTON I	100.00%
235_BOS	235_BOSTON	98.67%
245_LA	245_LOS ANGELES	98.67%
246_PEN	246_PENSACOLA	98.06%
256_JOL	256_LA JOLLA (SCRIPPS PIER)	97.34%
265_AST	265_ASTORIA (TONGUE POINT)	100.00%
311_ANN	311_ANNAPOLIS (NAVAL ACADEMY)	95.04%
332_EAST	332_EASTPORT	91.66%
351_NEW	351_NEWPORT	98.55%
360_WAS	360_WASHINGTON DC	97.82%
366_SAN	366_SANDY HOOK	97.82%
367_WOO	367_WOODS HOLE (OCEAN. INST.)	93.23%
378_CRES	378_CRESCENT CITY	98.43%
384_FRI	384_FRIDAY HARBOR (OCEAN. LABS.)	97.82%
385_NEA	385_NEAH BAY	97.34%
395_FOR	395_FORT PULASKI	98.55%
396_WIL	396_WILMINGTON	98.18%
405_JUN	405_JUNEAU	100.00%
412_SOL	412_SOLOMONS ISLAND (BIOL. LAB.)	95.29%
426_SIT	426_SITKA	99.39%
428_CED	428_CEDAR KEY II	94.44%
429_NL	429_NEW LONDON	95.89%
437_ALA	437_ALAMEDA (NAVAL AIR STATION)	99.27%
445_YAK	445_YAKUTAT	95.89%
497_ISA	497_PORT ISABEL	96.01%
508_LUIS	508_PORT SAN LUIS	94.20%
519_MON	519_MONTAUK	91.42%
520_PET	520_ST. PETERSBURG	99.87%
526_GRA	526_GRAND ISLE	95.41%

$$(1-B)^d x_t = x_t - dx_{t-1} + \frac{d(d-1)}{2}x_{t-2} - \dots,$$

so that the second equation in (2) can be expressed as:

$$x_t = dx_{t-1} - \frac{d(d-1)}{2}x_{t-2} + \dots + u_t$$

In this context, if d is a fractional value, x_t depends on all its past history and the higher the value of d is, the higher the level of dependence between the observations is. Moreover, if $d=0$, x_t exhibits short memory or $I(0)$ (in our case following a seasonal AR(1) process), while $d>0$ implies long memory, and a high level of time dependence in the data (Table 1).

For the estimation of the parameters in Eq. (2), we use a Whittle function in the frequency domain following the testing approach of Robinson (1994). This method has several advantages compared with other methods. First, it allows to test any real value of d, including those outside the stationary region ($d \geq 0.5$), without any need for the prior differentiation of the series required by most standard procedures. Secondly, the limit distribution is standard normal, unlike in the case of unit root methods when Monte Carlo simulations have to be carried out to examine the distribution of the tests. In addition, this limit distribution is not affected by the inclusion of deterministic terms or by the specification of the error term (see Gil-Alana and Robinson (1997) for a description of the version of the tests of Robinson (1994) used in this application).

Results

Table 2 displays the estimated values of d from Eq. (2) under three different assumptions:

i. no deterministic components, i.e., imposing $\alpha = \beta = 0$
ii. a constant only, i.e., with $\beta = 0$
iii. a constant and a linear time trend

Along with the estimated values of d, which are a measure of persistence, we also report their 95% confidence bands, which correspond exactly to the band of non-rejection values calculated as in Robinson (1994); the coefficients in bold are those from our preferred specification, which has been selected on the basis of the statistical significance of the deterministic terms; these are also reported in Table 3 together with the estimated α (constant), β (time trend coefficient) and ρ (seasonality). Note that the two first equations in (2) can be expressed as

$$\tilde{y}_t = \alpha \tilde{1}_t + \beta \tilde{t}_t + u_t,$$

where $\tilde{y}_t = (1 - L)^d y_t$; $\tilde{1}_t = (1 - L)^d 1$, and $\tilde{t}_t = (1 - L)^d t$, and noting that ut is $I(0)$ by assumption, standard t-tests apply here.

It can be seen from Table 2 that significant time trends are found in 29 cases out of 41; of those, only in four cases (Neah Bay, Juneau, Sitka and Yakutat) the trend is negative, being otherwise positive, with the estimated coefficient ranging from 0.158 (Portland Maine) to 0.745 (Grand Isle). The four stations with a negative trend are located on the North West coast, whilst those with a positive trend (25) are located on the East coast and the Gulf of Mexico; the 12 stations with an insignificant trend are all on the West coast (see Table 4 and Fig. 1). This evidence confirms the important role played by geographical location in the determination of the sea level.

Table 2 Estimates of d in the model given by equation (*)

Series	No deterministic terms	An intercept	An intercept and a linear time trend
10_SF	0.99 (0.94, 1.04)	**0.58 (0.51, 0.66)**	0.58 (0.51, 0.66)
12_NY	0.98 (0.93, 1.03)	0.40 (0.34, 0.47)	**0.38 (0.31, 0.47)**
112_FEB	0.96 (0.91, 1.02)	0.33 (0.26, 0.41)	**0.32 (0.24, 0.42)**
127_STT	0.97 (0.93, 1.03)	**0.42 (0.35, 0.52)**	0.42 (0.34, 0.52)
135_PHI	0.97 (0.92, 1.03)	0.39 (0.32, 0.46)	**0.37 (0.30, 0.46)**
148_BAL	0.97 (0.92, 1.03)	0.32 (0.26, 0.40)	**0.30 (0.22, 0.38)**
155_HON	0.99 (0.94, 1.04)	**0.74 (0.66, 0.83)**	0.74 (0.66, 0.83)
158_SDG	1.00 (0.95, 1.05)	**0.73 (0.66, 0.83)**	0.73 (0.66, 0.83)
180_ATL	0.98 (0.93, 1.03)	0.37 (0.33, 0.43)	**0.33 (0.26, 0.41)**
183_POR	0.99 (0.94, 1.04)	0.39 (0.34, 0.45)	**0.38 (0.33, 0.45)**
188_KW	0.99 (0.94, 1.04)	0.39 (0.32, 0.49)	**0.39 (0.29, 0.49)**
225_KET	0.99 (0.94, 1.05)	**0.40 (0.30, 0.51)**	0.40 (0.30, 0.51)
234_CHA	0.98 (0.93, 1.04)	0.37 (0.30, 0.45)	**0.36 (0.28, 0.46)**
235_BOS	0.98 (0.94, 1.04)	0.38 (0.33, 0.43)	**0.34 (0.28, 0.41)**
245_LA	1.00 (0.95, 1.05)	**0.69 (0.60, 0.78)**	0.69 (0.60, 0.78)
246_PEN	0.97 (0.92, 1.02)	0.47 (0.39, 0.56)	**0.47 (0.39, 0.56)**
256_JOL	1.00 (0.95, 1.05)	**0.75 (0.66, 0.85)**	0.75 (0.66, 0.85)
265_AST	0.96 (0.91, 1.02)	**0.44 (0.35, 0.53)**	0.44 (0.35, 0.53)
311_ANN	0.97 (0.92, 1.03)	0.33 (0.27, 0.40)	**0.29 (0.22, 0.38)**
332_EAST	0.99 (0.95, 1.04)	0.34 (0.31, 0.38)	**0.30 (0.27, 0.35)**
351_NEW	0.99 (0.94, 1.03)	0.39 (0.34, 0.46)	**0.36 (0.29, 0.45)**
360_WAS	0.96 (0.92, 1.02)	0.37 (0.31, 0.44)	**0.36 (0.27, 0.44)**
366_SAN	0.98 (0.93, 1.03)	0.38 (0.33, 0.44)	**0.34 (0.27, 0.42)**
367_WOO	0.98 (0.94, 1.04)	0.39 (0.34, 0.46)	**0.36 (0.29, 0.44)**
378_CRES	0.97 (0.93, 1.03)	**0.45 (0.37, 0.54)**	0.45 (0.37, 0.54)
384_FRI	0.97 (0.93, 1.03)	**0.43 (0.35, 0.53)**	0.43 (0.35, 0.53)
385_NEA	0.97 (0.92, 1.03)	0.37 (0.28, 0.47)	**0.36 (0.26, 0.47)**
395_FOR	0.98 (0.93, 1.04)	0.37 (0.30, 0.45)	**0.36 (0.28, 0.46)**
396_WIL	0.98 (0.93, 1.04)	0.42 (0.36, 0.51)	**0.42 (0.35, 0.52)**
405_JUN	0.99 (0.94, 1.05)	0.54 (0.49, 0.61)	**0.47 (0.39, 0.57)**
412_SOL	0.97 (0.93, 1.03)	0.33 (0.28, 0.39)	**0.28 (0.22, 0.37)**
426_SIT	1.00 (0.95, 1.06)	0.43 (0.35, 0.54)	**0.41 (0.32, 0.53)**
428_CED	0.97 (0.92, 1.03)	0.38 (0.31, 0.46)	**0.36 (0.29, 0.46)**
429_NL	0.98 (0.94, 1.04)	0.37 (0.32, 0.43)	**0.33 (0.27, 0.41)**
437_ALA	0.99 (0.94, 1.04)	**0.60 (0.53, 0.68)**	0.60 (0.53, 0.68)
445_YAK	0.99 (0.94, 1.05)	0.46 (0.40, 0.54)	**0.40 (0.32, 0.50)**
497_ISA	0.96 (0.91, 1.02)	0.40 (0.34, 0.48)	**0.39 (0.32, 0.47)**
508_LUIS	0.99 (0.95, 1.05)	**0.64 (0.56, 0.72)**	0.64 (0.56, 0.72)
519_MON	0.98 (0.93, 1.03)	0.38 (0.33, 0.44)	**0.33 (0.27, 0.41)**
520_PET	0.98 (0.93, 1.03)	0.41 (0.33, 0.50)	**0.40 (0.32, 0.50)**
526_GRA	0.96 (0.91, 1.02)	0.49 (0.44, 0.56)	**0.46 (0.39, 0.55)**

The values in parenthesis are the 95% confidence band of the non-rejection values of d; those in bold are the estimates for the preferred model specification

All the estimated values of d are in the interval (0, 1) and range between 0.29 (Annapolis, Naval Academy) and

Table 3 Estimated coefficients for the selected models

Series	d	β_0	β_1	Month AR1
10_SF	0.58 (0.51, 0.66)	6968.52 (180.66)	–	0.299
12_NY	0.38 (0.31, 0.47)	6912.04 (229.39)	0.295 (4.50)	0.401
112_FEB	0.32 (0.24, 0.42)	7120.09 (196.89)	0.232 (3.09)	0.631
127_STT	0.42 (0.34, 0.52)	7054.24 (187.79)	–	0.321
135_PHI	0.37 (0.30, 0.46)	6834.76 (186.85)	0.312 (3.96)	0.421
148_BAL	0.30 (0.22, 0.38)	6958.76 (249.17)	0.281 (4.92)	0.648
155_HON	0.74 (0.66, 0.83)	6994.76 (190.57)	–	0.263
158_SDG	0.73 (0.66, 0.83)	6930.84 (168.67)	–	0.544
180_ATL	0.33 (0.26, 0.41)	6898.44 (273.34)	0.396 (7.54)	0.430
183_POR	0.38 (0.33, 0.45)	7036.76 (360.68)	0.158 (3.72)	0.126
188_KW	0.39 (0.29, 0.49)	7071.00 (235.41)	0.235 (3.55)	0.645
225_KET	0.40 (0.30, 0.51)	7043.24 (208.50)	–	0.399
234_CHA	0.36 (0.28, 0.46)	6948.46 (192.78)	0.301 (3.92)	0.565
235_BOS	0.34 (0.28, 0.41)	7011.35 (387.37)	0.241 (6.33)	0.147
245_LA	0.69 (0.60, 0.78)	6964.45 (177.70)	–	0.522
246_PEN	0.47 (0.39, 0.56)	6985.20 (158.20)	0.230 (2.07)	0.615
256_JOL	0.75 (0.66, 0.85)	6903.54 (163.29)	–	0.525
265_AST	0.44 (0.35, 0.53)	6968.30 (152.90)	–	0.399
311_ANN	0.29 (0.22, 0.38)	6885.08 (268.55)	0.325 (6.21)	0.663
332_EAST	0.30 (0.27, 0.35)	6957.11 (581.35)	0.180 (7.37)	0.112
351_NEW	0.36 (0.29, 0.45)	6998.48 (345.11)	0.259 (5.99)	0.365
360_WAS	0.36 (0.27, 0.44)	6829.83 (180.31)	0.327 (4.05)	0.415
366_SAN	0.34 (0.27, 0.42)	6940.46 (273.27)	0.365 (6.84)	0.407
367_WOO	0.36 (0.29, 0.44)	6917.40 (355.40)	0.278 (6.70)	0.360
378_CRES	0.45 (0.37, 0.54)	7087.58 (199.54)	–	0.353
384_FRI	0.43 (0.35, 0.53)	7030.04 (213.89)	–	0.316
385_NEA	0.36 (0.26, 0.47)	7073.09 (170.64)	−0.175 (−1.98)	0.472
395_FOR	0.36 (0.28, 0.46)	6990.50 (180.06)	0.318 (3.84)	0.586
396_WIL	0.42 (0.35, 0.52)	6988.23 (186.49)	0.297 (3.45)	0.313
405_JUN	0.47 (0.39, 0.57)	7132.96 (137.97)	−1.027 (−7.88)	0.224
412_SOL	0.28 (0.22, 0.37)	6978.77 (306.59)	0.348 (7.53)	0.612
426_SIT	0.41 (0.32, 0.53)	7037.94 (159.46)	−0.172 (−1.72)	0.436
428_CED	0.36 (0.29, 0.46)	6934.56 (230.15)	0.212 (3.29)	0.700
429_NL	0.33 (0.27, 0.41)	6949.22 (356.43)	0.254 (6.26)	0.394
437_ALA	0.60 (0.53, 0.68)	7001.56 (178.94)	–	0.273
445_YAK	0.40 (0.32, 0.50)	7025.33 (152.11)	−0.684 (−6.63)	0.447
497_ISA	0.39 (0.32, 0.47)	6934.30 (185.98)	0.354 (4.31)	0.616
508_LUIS	0.64 (0.56, 0.72)	6969.98 (180.63)	–	0.506
519_MON	0.33 (0.27, 0.41)	6992.81 (365.32)	0.302 (7.61)	0.380
520_PET	0.40 (0.32, 0.50)	7005.62 (228.36)	0.256 (3.75)	0.667
526_GRA	0.46 (0.39, 0.55)	6735.09 (155.02)	0.745 (6.95)	0.620

The values in parenthesis in the third and fourth columns refer to the corresponding t-values; values higher than 1.64 indicate significance of the estimated coefficients

Table 4 Classification based on the time trend coefficient

Significant negative time trend		Insignificant time trend	Significant positive time trend	
405_JUN	(−1.027)	10_SF	183_POR	(0.158)
445_YAK	(−0.684)	127_STT	332_EAST	(0.180)
385_NEA	(−0.175)	155_HON	428_CED	(0.212)
426_SIT	(−0.172)	158_SDG	246_PEN	(0.230)
		225_KET	112_FEB	(0.232)
		245_LA	188_KW	(0.235)
		256_JOL	235_BOS	(0.241)
		265_AST	429_NL	(0.254)
		378_CRES	520_PET	(0.256)
		384_FRI	351_NEW	(0.259)
		437_ALA	367_WOO	(0.278)
		508_LUIS	148_BAL	(0.281)
			12_NY	(0.295)
			396_WIL	(0.297)
			234_CHA	(0.301)
			519_MON	(0.302)
			135_PHI	(0.312)
			395_FOR	(0.318)
			311_ANN	(0.325)
			360_WAS	(0.327)
			412_SOL	(0.348)
			497_ISA	(0.354)
			366_SAN	(0.365)
			180_ATL	(0.396)
			526_GRA	(0.745)

0.75 (La Jolla, Scripps Piers), which confirms that the series are fractionally integrated and supports the hypothesis of long-memory behaviour. The series can be divided into three categories according to their degree of persistence: those with values of d in the range (0, 0,5), that is, covariance-stationary series; those with values around 0.5, on the boundary between stationarity and non-stationarity; a third group with values in the interval [0.5, 1), which implies non-stationary mean-reverting behaviour (see Table 5 and Fig. 2).

It can be seen that 22 stations are in the first category with a low degree of persistence, and virtually all of them are located on the East coast; for 12 stations the estimated value of d implies that they belong to the intermediate category, and these are all located on the Gulf of Mexico or the West coast; 7 stations are in the non-stationary range ($d \geq 0.5$), all them on the West coast, and since the estimated value of d is in all cases significantly below 1 mean-reversion occurs, with the effects of shocks dying away in the long run. The estimated degree of persistence is an important piece of information which reveals that, following a shock, the speed of the dynamic adjustment towards the initial equilibrium level is highest in the case of the East coast stations and lowest for some West coast and Gulf of Mexico stations, whilst it is in the middle of the estimated range for some other West coast ones. The implication is that intervention to restore the equilibrium level is most needed on the West coast and the Gulf of Mexico.

Conclusions

This paper examines US sea level data for a set of 41 stations chosen on the basis of data availability and covering most of the US coastline. A fractional integration framework is applied to test for the presence of trends and the degree of persistence. The results indicate that all series are fractionally integrated, since their differencing parameter is estimated to lie in the interval (0, 1). More specifically, there is evidence of long-memory stationarity (i.e., $0 < d < 0.5$) for 22 stations, most of them located on the East coast; for 12 stations the order of integration is around 0.5, and for 7 (all located on the West coast) there is evidence of non-stationary mean-reverting patterns ($0.5 \leq d < 1$).

There are significant time trends in 29 out of the 41 cases examined (positive in 25 cases and negative in 4). The stations with a positive trend are located on the East coast and the Gulf of Mexico, while the four with a negative trend (Neah Bay, Juneau, Sitka and Yakutat) are located on the North West coast. These findings imply that there is a clear rise in the US sea level only in the case the East coast and the Gulf of Mexico, and therefore the authorities should focus on those to address the issue of an increasing sea level. This conclusion is also corroborated by the estimated degree of persistence, which is higher for the West coast stations, suggesting that the effects of shocks will be more long-lived in their case.

Future work could extend the analysis of this paper. For example, the possibility of nonlinear (time) trends would be worth investigating since fractional integration is intimately related with non-linearities and possible breaks in the data (Granger and Hyung, 2004; Ohanissian et al. 2008; etc.). In addition, an alternative modelling approach could be used allowing for fractional or persistent cycles since long memory is a property of the data not necessarily limited to processes with the singularity or pole in the spectrum occurring at the zero frequency.

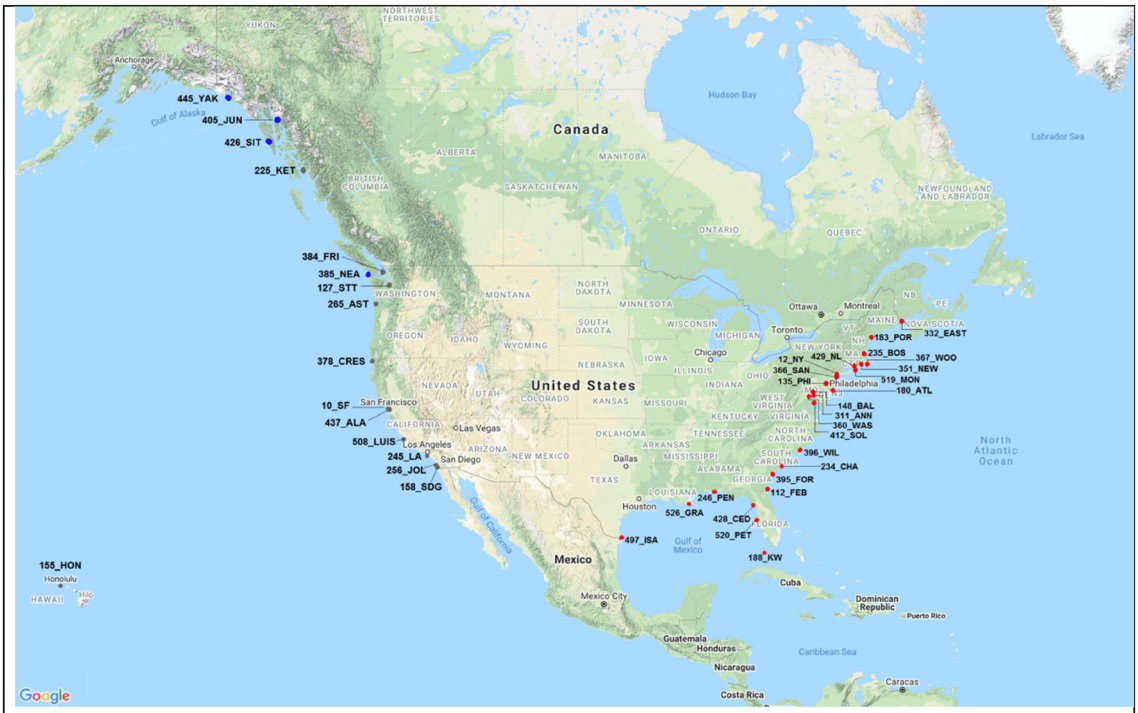

• Significant positive time trend; • Insignificant time trend; • Significant negative time trend.

Fig. 1 Time trend coefficients. Summary of data extracted from Table 4

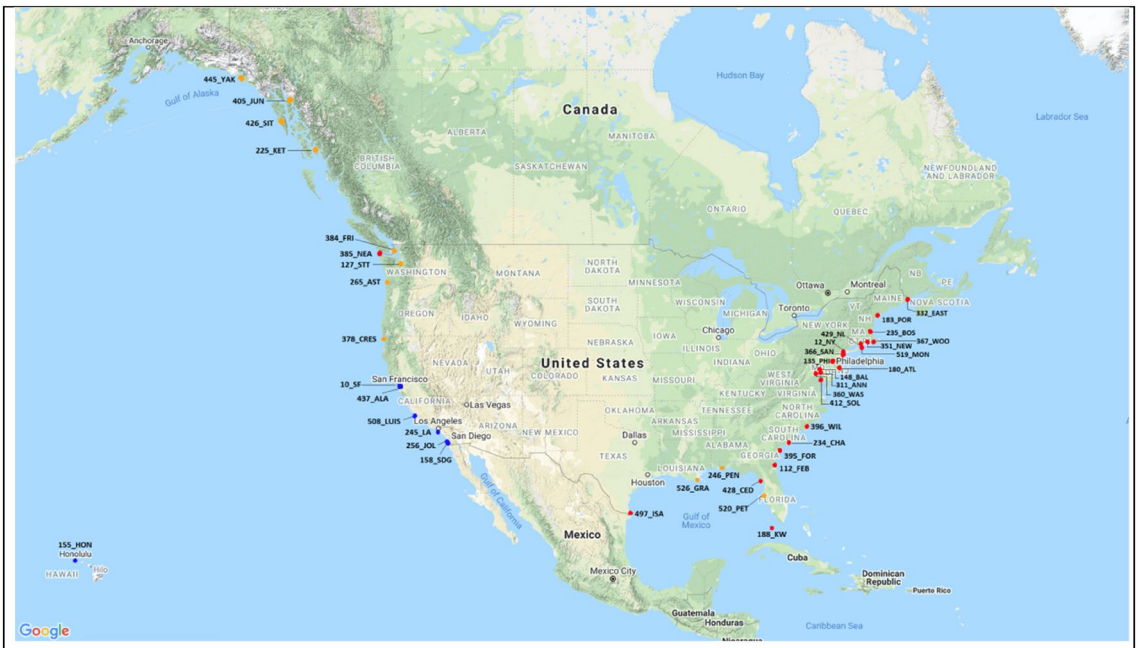

• $d < 0.4$; • $0.40 \leq d < 0.5$; • $d > 0.5$.

Fig. 2 Degree of persistence. Summary of data extracted from Table 5

Table 5 Classification based on persistence

$0 < d < 0.5$ Stationarity		$0 < d < 1$ $(0.40 < d < 0.50)$		$0.5 \le d < 1$ Non-stationarity	
412_SOL	(0.28)	225_KET	(0.40)	10_SF	(0.58)
311_ANN	(0.29)	445_YAK	(0.40)	437_ALA	(0.60)
148_BAL	(0.30)	520_PET	(0.40)	508_LUIS	(0.64)
332_EAST	(0.30)	426_SIT	(0.41)	245_LA	(0.69)
112_FEB	(0.32)	127_STT	(0.42)	158_SDG	(0.73)
180_ATL	(0.33)	396_WIL	(0.42)	155_HON	(0.74)
429_NL	(0.33)	384_FRI	(0.43)	256_JOL	(0.75)
519_MON	(0.33)	265_AST	(0.44)		
366_SAN	(0.34)	378_CRES	(0.45)		
235_BOS	(0.34)	526_GRA	(0.46)		
385_NEA	(0.36)	246_PEN	(0.47)		
360_WAS	(0.36)	405_JUN	(0.47)		
234_CHA	(0.36)				
395_FOR	(0.36)				
367_WOO	(0.36)				
351_NEW	(0.36)				
428_CED	(0.36)				
135_PHI	(0.37)				
12_NY	(0.38)				
183_POR	(0.38)				
188_KW	(0.39)				
497_ISA	(0.39)				

The header in this table refers to the significant cases. For example, although all the values appearing in the second column are in the interval (0.4, 0.5), their confidence intervals include some values in the range (0, 0.5) and others in the range [0.5, 1)

Acknowledgements Prof. Luis A. Gil-Alana gratefully acknowledges financial support from the MINEIC-AEI-FEDER ECO2017-85503-R project from 'Ministerio de Economía, Industria y Competitividad' (MINEIC), `Agencia Estatal de Investigación' (AEI) Spain and `Fondo Europeo de Desarrollo Regional' (FEDER). He also acknowledges support from an internal project of the Universidad Francisco de Vitoria. In addition, we wish to thank Jose Juan Toscano for help with the figures.

Authors contribution GMC has contributed with the literature review, the interpretation of the results and concluding comments. LAG-A has contributed with the introduction, the methodology, the codes and interpretation of the results. LS has contributed with the original idea, introduction and concluding section.

Funding Open Access funding provided thanks to the CRUE-CSIC agreement with Springer Nature. Open Access funding provided thanksto the CRUE-CSIC agreement with Springer Nature.

Availability of data and materials Data are available for the authors upon request.

Declarations

Competing interest There are no competing interests with the publication of the present manuscript.

Ethical approval There are no ethical issues dealing with the present manuscript.

Consent to participate There is consent to participate the authors in the manuscript.

Consent to publish There is consent to the publication of the manuscript.

References

Barbosa SM, Silva ME, Fernandes MJ (2008) Time series analysis of sea-level records: characterising long-term variability. In: Donner RV, Barbosa SM (eds) Nonlinear time series analysis in the geosciences. Lecture Notes in Earth Sciences, 112, 157–173.

Becker M, Karpytchev M, Lennartz-Sassinek S (2014) Long-term sea level trends: Natural or anthropogenic? Geophys Res Lett 41(15):5571–5580

Beran J (1994) Statistics for long-memory processes. Chapman & Hall, New York, pp 1–315
Bloomfield P (1992) Trends in global temperatures. Clim Change 21(1):275–287
Boon JD (2012) Evidence of sea level acceleration at US and Canadian tide stations, Atlantic coast, North America. J Coast Res 28(6):1437–1445
Boon JD, Mitchell M (2015) Nonlinear change in sea level observed at North American tide stations. J Coastal Res 31(6):1295–1305
Bos MS, Williams SDP, Araujo IB, Bastos L (2014) The effect of temporal correlated noise on the sea level rate and acceleration uncertainty. Geophys J Int 196(3):1423–1430
Bunde A (2017). In: Christian L, Franzke E, Okane T (eds) Long-term memory in climate: Detection, extreme events and significance of trends, Chapter 11 Nonlinear and Stochastic Climate Dynamics. Cambridge University Press, Cambridge
Caballero R, Jewson S, Brix A (2002) Long memory in surface air temperature: detection, modelling, and application to weather derivative valuation. Clim Res 21(2):127–140
Chandler RE, Scott EM (2011) Statistical methods for trend detection and analysis in the environmental science. John Wiley & Sons Ltd, New York, pp 1–368
Church JA, Gregory JM (2019) Sea level change reference module in earth systems and environmental sciences. Encycl Ocean Sci (third Edition) 6:493–499
Church JA, White NJ (2006) A 20th century acceleration in global sea-level rise. Geophys Res Lett 33(1):L01602
Church JA, Gregory JM, Huybrechts P, Kuhn M, Lambeck K, Nhuan MT, Qin D, Woodworth PL (2001) Changes in sea level. In: Houghton JT, Ding Y, Griggs DJ, Noguer M, van der Linden PJ, Dai X, Maskell K, Johnson CA (eds) Climate change 2001: the scientific basis. Contribution of working group I to the third assessment report of the intergovernmental panel on climate change. Cambridge University Press, Cambridge, p 881
Church J, Clark P, Cazenave A, Gregory J, Jevrejeva S, Levermann A, Merrifield M, Milne G, Nerem R, Nunn P, Payne A, Pfeffer W, Stammer D, Alakkat U (2013) In: Climate change 2013: the physical science basis. Contribution of working group I to the fifth assessment report of the intergovernmental panel on climate change. Sea level change. Pp 1138–1191
Dangendorf S, Rybski D, Mudersbach C, Müller A, Kaufmann E, Zorita E, Jensen J (2014) Evidence for long-term memory in sea level. Geophys Res Lett 41(15):5530–5537
Dangendorf S, Marcos M, Muller A, Zorita E, Riva R, Berk K, Jensen J (2015) Detecting anthropogenic footprints in sea level rise. Nat Commun 6(1):1–9
Dangendorf S et al (2017) 2017, Reassessment of 20th century global mean sea level rise. Proc Natl Acad Sci 114:5946–5951
Ercan A, Kavvas ML, Abbasov RK (2013) Long-range dependence and sea level forecasting. Springer International Publishing, Berlin, pp 1–51
Franzke C (2012) Nonlinear trends, long-range dependence, and climate noise properties of surface temperature. J Clim 25(12):4172–4183
Gil-Alana LA (2005) Statistical model for the temperatures in the Northern hemisphere using fractional integration techniques. J Clim 18(24):5537–5369
Gil-Alana LA (2006) Nonstationary, long memory and antipersistence in several climatological time series data. Environ Model Assess 11(1):19–29
Gil-Alana LA (2008) Time trend estimation with breaks in temperature time series. Clim Change 89(3–4):325–337
Gil-Alana LA (2015) Linear and segmented trends in sea surface temperature data. J Appl Stat 42(7):1531–1546
Gil-Alana LA (2017) Alternative modelling approaches for the ENSO time series. Persistence and seasonality. Int J Climatol 37(5):2354–2363
Gil-Alana LA (2018) Maximum and minimum temperatures in the United States: time trends and persistence. Atmos Sci Lett 19(4):810–813
Gil-Alana LA, Robinson PM (1997) Testing of unit roots and other nonstationary hypotheses in macroeconomic time series. J Econ 80(2):241–268
Granger CWJ, Hyung N (2004) Occasional structural breaks and long memory with an application to the S&P 500 absolute stock returns. J Empir Financ 11:399–421
Granger CWJ, Joyeux R (1980) An introduction to long memory time series models and fractional differencing. J Time Ser Anal 1(1):15–29
Graves T, Gramacy R, Watkins N, Franzke C (2017) A brief history of long memory: hurst, Mandelbrot and the road to ARFIMA 1951–1980. Entropy 19(9):1–21
Holgate SJ, Matthews A, Woodworth PL, Rickards LJ, Tamisiea ME, Bradshaw E, Foden PR, Gordon KM, Jevrejeva S, Pugh J (2013) New data systems and products at the permanent service for mean sea level. J Coastal Res 29(3):493–504. https://doi.org/10.2112/JCOASTRES-D-12-00175.1
Houston J, Dean R (2011) Sea-level acceleration based on US tide gauges and extensions of previous global-gauge analysis. J Coast Res 27(3):409–417
Hsui AT, Rust KA, Klein GD (1993) A fractal analysis of quaternary, cenozoic-mesozoic, and late pennsylvanian sea level changes. J Geophys Res 98(B12):21963–21967
Hurst HE (1951) Long-term storage capacity of reservoirs. Trans Am Soc Civ Eng 116(1):770–799
Jevrejeva S, Grinsted A, Moore JC (2009) Anthropogenic forcing dominates sea level rise since 1850. Geophys Res Lett 36(L20706):1–5
Jevrejeva S, Moore JC, Grinsted A, Matthews AP, Spada G (2014) Trends and acceleration in global and regional sea levels since 1807. Global Planet Change 113:11–22
Jiang J, Plotnick RE (1998) Fractal analysis of the complexity of United States Coastlines. Math Geol 30(5):535–546
Kantelhardt JW, Kocielny-Bunde E, Rego HA, Havlin S, Bunde A (2001) Detecting long-range correlations with detrended fluctuation analysis. Phys A 295(3–4):441–454
Koop RE (2013) Does the mid-Atlantic United States sea level acceleration hot spot reflect ocean dynamic variability? Geophys Res Lett 40(15):3981–3985
Kulp SA, Strauss BH (2019) New elevation data triple estimates of global vulnerability to sea-level rise and coastal flooding. Nat Commun 10:4844. https://doi.org/10.1038/s41467-019-12808-z
Lennartz S, Bunde A (2012) On the estimation of natural and anthropogenic trends in climate records Washington DC American geophysical union. Geophys Monogr Ser 196:177–189
Mandelbrot B (1967) How long is the coast of britain? Statistical self-similarity and fractional dimension. Science 155(3775):636–638
Mandelbrot B (1982) The Fractal Geometry of Nature. W. H, Freeman and Company, New York
Mandelbrot BB, van Ness JW (1968) Fractional Brownian motions, fractional noises and applications. SIAM Rev 10(4):422–437
Marcos M, Marzeion B, Dangendorf S, Slangen ABA, Palanisamy H, Fenoglio-Marc L (2016) Internal variability versus anthropogenic forcing on sea level and its components. Surv Geophys 38(1):329–348
Mudelsee M (2010) Climate time series analysis. Classical statistical and bootstrap methods, 2nd edn. Springer, Dordrecht
Ohanissinan A, Russell JR, Tsay RS (2008) True or spurious long memory? A new test. J Bus Econ Stat 26:161–175

Oppenheimer M, Glavovic BC, Hinkel J, van de Wal R, Magnan AK, Abd-Elgawad A, Cai R, Cifuentes-Jara M, DeConto RM, Ghosh T, Hay J, Isla F, Marzeion B, Meyssignac B, Sebesvari Z (2019) Sea level rise and implications for low-lying islands, coasts and communities. In: IPCC Special Report on the Ocean and Cryosphere in a Changing Climate, 321–446.

Parris A, Bromirski P, Burkett V, Cayan D, Culver M, Hall J, Horton R, Knuuti K, Moss R, Obeysekera J, Sallenger A, Weiss J (2012) Global sea level rise scenarios for the US national climate assessment. NOAA Tech Memo OAR CPO-1, p 37

Percival DB, Overland JE, Mofjeld HO (2001) Interpretation of North Pacific variability as a short- and long-memory process. J Clim 14(24):4545–4559

Permanent Service for Mean Sea Level (PSMSL), 2019, "Tide Gauge Data", Retrieved 05 Dic 2019 from http://www.psmsl.org/data/obtaining/.

Restrepo-Ángel JD, Mora-Páez H, Díaz F et al (2021) Coastal subsidence increases vulnerability to sea level rise over twenty first century in Cartagena Caribbean Colombia. Sci Rep 11:18873. https://doi.org/10.1038/s41598-021-98428-4

Robinson PM (1994) Efficient tests of nonstationary hypotheses. J Am Stat Assoc 89(428):1420–1437

Royston S, Watson CS, Legrésy B, King MA, Church JA, Bos MS (2018) Sea-level trend uncertainty with Pacific climatic variability and temporally-correlated noise. J Geophys Res Oceans 123(3):1978–1993

Slangen ABA, Church JA, Agosta C, Fettweis X, Marzeion B, Richter K (2016) Anthropogenic forcing dominates global mean sea-level rise since 1970. Nat Clim Chang 6:701–705

Sweet WV, Kopp RE, Weaver CP, Obeyskera J, Horton RM, Thieler ER, Zervas C (2017) Global and regional sea level rise scenarios for the United States, NOAA Technical Report NOS CO-OPS083.

Visser H, Dangendorf S, Petersen AC (2015) A review of trend models applied to sea level data with reference to the "acceleration-deceleration debate. J Geophys Res Oceans 120(6):3873–3895

Warrick RA, Oerlemans J (1990) Sea level rise. In: Houghton JT, Jenkins GJ, Ephraum JJ (eds) Climate change: the IPCC scientific assessment. Cambridge University Press, Cambridge, pp 260–281

Watson PJ (2016) Acceleration in US mean sea level? A new insight using improved tools. J Coast Res 32(6):1247–1261

WCRP Global Sea Level Budget Group (2018) Global sea level budget 1993-present. Earth Syst Sci Data 10(3):1551–1590

Woodworth PL, White NJ, Jevrejeva S, Holgate SJ, Church JA, Gehrels WR (2009) Evidence for the accelerations of sea level rise on multi-decade and century timescales. Int J Climatol 29(6):777–789

Yuan N, Fu Z, Liu S (2013) Long-term memory in climate variability: A new look based on fractional integral techniques. J Geophys Res Atmos 118(12):962–969

Yuan N, Huang Y, Duan J, Zhu C, Xoplaki E, Luterbacher J (2019) On climate prediction; how much can we expect from climate memory? Clim Dyn 52(1–2):855–864

Zemunik P, Šepić J, Pellikka H, Ćatipović L, Vilibić I (2021) Minute sea-level analysis (MISELA): a high-frequency sea-level analysis global dataset. Earth Syst Sci Data 13:4121–4132. https://doi.org/10.5194/essd-13-4121-2021

Zervas C (2009) Sea level variations of the United States 1854–2006, NOAA Technical Report NOS CO-OPS 053